Invited Research Article

SIMS oxygen isotope matrix effects in silicate glasses: Quantifying the role of chemical composition

Elena Dubinina [a],[*], Alexander Borisov [a], Michael Wiedenbeck [b], Alexander Rocholl [b]

[a] Institute of Geology of Ore Deposits, Petrography, Mineralogy and Geochemistry Russian Academy of Sciences, Staromonetnyi pereulok 35, 109017 Moscow, Russia
[b] Deutsches GeoForschungsZentrum GFZ, Telegrafenberg, D-14473 Potsdam, Germany

ARTICLE INFO

ABSTRACT

Instrumental mass fractionation (IMF) associated with Secondary Ion Mass Spectrometry (SIMS) measurements of oxygen isotope compositions in silicate glasses was studied using a set of 27 synthesized glasses spanning a compositionally broad range of six major oxides: SiO_2, TiO_2, Al_2O_3, total FeO (FeO_t), MgO and CaO. The impact of chemical composition on the IMF values was investigated using a Cameca 1280-HR during a single SIMS analytical session operated under constant instrumental conditions. The data measured were compared with the $\delta^{18}O$ values obtained by laser fluorination gas source mass-spectrometry (LF). The offset between the $\delta^{18}O(LF)$ and $\delta^{18}O(SIMS)$ was found to reach up to 5‰. Our data document that SIMS oxygen isotope matrix effects in silicate glasses strongly depend on the chemical composition of silicate glasses, here the cation-oxygen bond strength was found to have a strong influence on the IMF value. We tested a variety of models based on single oxide contents and various composition-dependent parameters, but none were fully satisfactory for predicting IMF. Neither mean atomic mass nor NBO/T (the ratio of non-bridging oxygens per tetrahedrally coordinated cation) show a strong correlation with the IMF values (R^2 of 0.45 and 0.46, respectively). Among the single oxides, only the model based on the SiO_2 content is useful for prediction of the IMF in silicate glasses, but this model has a large standard error ($1\sigma = \pm 0.90$‰) and was also found to break down for glasses with high Na and K contents. We propose an empirical model based on the correlation of six major element oxides that shows a strong correlation with IMF ($R^2 = 0.98$, $1\sigma = \pm 0.40$‰). This model describes the experimental data with uncertainties that are roughly a factor of two better than the correction methods proposed in earlier studies. We also investigated using the correlation between IMF and isotope I-^{18}O index, which describes the correlation between atomic bond strength and relative oxygen isotope enrichment in silicate substances ($R^2 = 0.87$). Although our efforts provide refinements to the SIMS determination of $\delta^{18}O$ in natural silicate glasses, truly accurate IMF corrections will need further refinements related to the impact of alkali elements.

1. Introduction

The oxygen isotope composition of silicate rocks and minerals is a powerful tool for investigating petrogenetic processes including the origin of silicate melts, the genesis of associated fluids, and the estimation of crystal solidification temperatures as well as providing key constraints on magma evolution caused by fractional crystallization, crustal contamination and magma degassing (see reviews by Valley, 2001; Eiler, 2001). Today, bulk analyses of microgram samples are performed by laser-based heating techniques (Sharp, 1990), providing $\delta^{18}O$ data quality with total uncertainties often better than ±0.1‰ (1 σ). However, many scientific applications today require spatial resolutions

of no more than a few 10s of micrometers, which is only possible by SIMS. For example, in magmatic silicate systems in situ determination of oxygen isotopes in phenocrysts, glasses and melt inclusions can be key for understanding the crystallization and/or eruption history of mantle generated melts (e.g., Bindeman, 2008).

SIMS can rapidly determine oxygen isotope composition at a spatial resolution <20 μm; with a slight reduction in data quality SIMS is even capable of providing determinations at ≤5 μm. A drawback of this technique is its critical dependence upon matrix matched reference materials. Instrumental mass fractionation (IMF) is critically dependent upon not only the atomic structure of the analyte (e.g., mineral phase vs. amorphous glass) but also on the major element chemistry of the

* Corresponding author.
  E-mail address: delta@igem.ru (E. Dubinina).

materials (Busch et al., 1983; Davies et al., 2018; Eiler et al., 1997; Fàbrega et al., 2017; Hartley et al., 2012; Hauri et al., 2002; Ickert and Stern, 2013; Ottolini et al., 2002; Page et al., 2010; Riciputi et al., 1998; Scicchitano et al., 2018). Here, for the case of oxygen isotope ratio determinations – the focus of this study – we define this factor as:

$$IMF = \left\{ \left[\left({}^{18}O/{}^{16}O \right)_{measured,SIMS} \middle/ \left({}^{18}O/{}^{16}O \right)_{measured,true} \right] - 1 \right\} \cdot 1000‰ \quad (1)$$

where $({}^{18}O/{}^{16}O)_{measured,true}$ is based on the "bulk" composition of the material as determined by gas source mass spectrometry.

The IMF value is the product of three components that, in the case of $\delta^{18}O$ determinations, are all close to unity: (1) the ratio between the ionization and extraction efficiencies of the two isotopes, (2) the ratio in the overall transmission efficiencies of the two ions within the mass spectrometer's flight tube, and (3) the ratio of small differences in detection efficiencies, be that when using a single counter in mono-collection mode or between two ion detectors used during static multi-collection mode. All three of these factors will vary depending on slight shifts in the precise analytical conditions (e.g., primary beam density at the point of impact, sample charging, beam centering on the entrance slit to the mass spectrometer, Faraday Cup background, etc.). Hence, there is a need to continually monitor IMF on an ongoing basis throughout a SIMS analytical session. The so-called "chemical matrix effect" is the result of shifts in the first of these factors; such shifts result from modifications to the relative ion yield between the two oxygen isotopes at the atomic scale. Much work has been devoted to understanding the SIMS matrix effect in geological materials (e.g., Hinton, 1995), but as yet no comprehensive model has been found for mathematically addressing this challenge. Beyond the major element chemistry of the analyte at the point of sputtering, during mineral analyses crystal orientation and sample surface topography may additionally influence the IMF (Eiler et al., 1997; Kita et al., 2009; Huberty et al., 2010). All these factors result in the so-called matrix effect, which was first observed for trace elements (Deline et al., 1978; Shimizu, 1986; Chakraborty, 1998; Ottolini et al., 2002) and later also for isotope ratio determinations (Eiler et al., 1997; Riciputi et al., 1998; Vielzeuf et al., 2005; Hauri et al., 2006; Rosner et al., 2008; Fukuda et al., 2020). Typically, the influence of sample chemistry on the IMF is addressed by using reference material with compositions and structure that "closely" match the analyte being investigated. The compositional effect for minerals with little to no chemical variability (e.g., quartz, zircon) can be easily addressed, whereas more complex minerals (garnet, feldspars, olivine, etc.) require more sophisticated calibrations. The role of matrix effect during SIMS oxygen isotope analyses has been studied for several mineral groups (Eiler et al., 1997; Vielzeuf et al., 2005; Ickert and Stern, 2013; Deegan et al., 2016; Davies et al., 2018; Sun et al., 2016; Fàbrega et al., 2017; Śliwiński et al., 2018). For example, a significant influence of the relative Fe and Mg contents in olivine on the IMF of oxygen isotopes has been reported by Isa et al. (2017). Similarly, a clear link between the Mg content and IMF has also been observed in Fe- and Mn-bearing carbonates (Rollion-Bard and Marin-Carbonne, 2011; Balestra et al., 2020).

Due to an effectively infinite compositional space, addressing SIMS matrix effects for isotopic determinations on silicate glasses can prove significantly more complex than in any of the above-mentioned mineral systems. To date only two studies of matrix effects in geological glasses have been reported. Eiler et al. (1997) found a positive correlation between IMF and mean atomic mass. They also proposed that the content of network-modifiers (i.e., Ca, Na, K, Fe, Mg, Mn and non-tetrahedral Al) can contribute towards differences in IMF for minerals and glasses with the similar chemical compositions. A second publication by Hartley et al. (2012) modeled the chemical matrix effect on a suite of silicate glass reference materials with compositions spanning from basalt to rhyolite. Based on SIMS $\delta^{18}O$ determinations on 12 glass materials, these authors showed that IMF corrections based on chemical composition is complex, leading them to investigate several correction schemes. They found the strongest correlations between IMF and SiO$_2$ (R^2 = 0.95–0.98) and CaO (R^2 = 0.88) contents. As a result, the univariate correction to SiO$_2$ or a bivariate correction using SiO$_2$-CaO or FeO-CaO content was recommended for correcting of SIMS $\delta^{18}O$ data obtained on natural glasses. However, other rock forming oxides can also influence IMF in silicate glasses, for example the network former TiO$_2$ or the network modifier MgO (Eiler et al., 1997). So, despite these earlier detailed investigations, the IMF correction for natural silicate glasses remains a challenge.

The research presented here aims to develop a refined algorithm for addressing the SIMS compositional matrix effect for $\delta^{18}O$ determinations on silicate glasses. We developed a suite of synthetic glasses covering a broad range of chemical compositions within the system SiO$_2$ + Al$_2$O$_3$ + FeO$_t$ ± CaO ± MgO ± TiO$_2$ (SAFCMT); several reference glasses with natural compositions were also included as part of this investigation. Previously we studied these SAFCMT glasses, including the determination of their chemical composition and oxygen isotope ratios with laser fluorination gas source mass spectrometry (GS-MS) (Dubinina and Borisov, 2018). All our synthetic glasses are free of gas inclusions and free of trace elements in their compositions, making it possible to limit our work to address only Si, Al, Fe, Ca, Mg and Ti. Because all our SIMS measurements were conducted during a single analytical session lasting 18 h with stable instrumental conditions, our experiment was optimized to assess the role of these major elements on IMF.

2. Materials and methods

2.1. SAFCMT glasses preparation

Twenty-seven glasses with SiO$_2$ + Al$_2$O$_3$ ± FeO$_t$ ± CaO ± MgO ± TiO$_2$ compositions were produced in a one atm vertical tube furnace with the loop technique at the Leibniz Universität Hannover, Institut für Mineralogie. A detailed description of this procedure is reported by Borisov and Dubinina (2014) and Dubinina and Borisov (2018). In brief: small Pt wire loop samples were equilibrated with the furnace gas (air or CO$_2$) at 1450–1550 °C. After air quenching, the pure glass samples were gently crushed and multiple fragments were mounted in epoxy resin and polished for EPMA analysis. Other fragments were used for oxygen isotope studies both by laser fluorination and SIMS with the Potsdam Cameca 1280-HR.

Four iron- and alkali-free 1 atm eutectic point compositions were chosen as base mixtures for preparing the SAFCMT glasses: diopside-anorthite eutectic (DA), enstatite-anorthite-silica eutectic (HR), SiO$_2$-Al$_2$O$_3$-MgO eutectic (HA) and silica-anorthite eutectic (SA), all modified with additional oxides (Table 1). Most of these mixtures were initially prepared to study the effects of melt composition on ferric/ferrous ratio (Borisov et al., 2013, 2015, 2017, 2018). The Fe^{3+}/Fe^{2+} ratio for iron-containing samples is given in Table 1.

These glasses were analyzed by SIMS in the single analytical session along with three reference MPI-DING glasses with natural compositions (rhyolite ATHO-G, basalt KL2-G and andesite StHs6/80-G) (Jochum et al., 2006). Additionally, the NIST certified reference material SRM 610 (NIST 610 glass) was also analyzed repeatedly during this session. Both the chemical compositions and $\delta^{18}O$ values of the ATHO-G, KL2-G and StHs6/80-G glasses were reported by Jochum et al. (2006). Additionally, chips of the MPI-DING glasses were reanalyzed as part of the present work using the laser fluorination GS-MS technique. The chemical composition of the NIST 610 glass has been reported by Hinton (1999) and Pearce et al. (1997). The data obtained with the Toronto EPMA (Pearce et al., 1997) are very close to data published in Hinton's work (1999) with the exception of SiO$_2$ contents which differ by nearly 1 wt%. For the calculations below the data of Hinton (1999) are used. For the $\delta^{18}O$ value of NIST 610 we used the value obtained by GS-MS technique reported by Kasemann et al. (2001). The bulk chemical compositions and $\delta^{18}O$ values for all of these reference materials are

Table 1

Chemical and oxygen isotope compositions of the synthetic glasses that were analyzed during a single session with the Potsdam Cameca 1280-HR ion microprobe.

Sample	Fe^{3+}/Fe^{2+}	Glass composition (EPMA) normalized to 100 wt%						Composition-dependent parameters			Oxygen isotope data (*)				IMF, ‰
		SiO_2	TiO_2	Al_2O_3	FeO_t	MgO	CaO	I-^{18}O	NBO/T	M.A.M.	$\delta^{18}O$ SIMS, ‰ drift-corrected	n	1σ, ‰	$\delta^{18}O$ LF, ‰	
DA-67	nd	50.60	0.00	15.70	0.00	10.10	23.60	0.807	0.900	21.99	16.73	8	0.15	12.73	**3.03**
DA-68	nd	50.60	0.00	15.70	0.00	10.10	23.60	0.807	0.900	21.99	16.02	8	0.11	12.26	**2.8**
DAF-77	1.94	46.10	0.00	14.25	8.91	9.20	21.53	0.785	0.701	22.97	26.33	7	0.06	22.6	**2.73**
DAF-5	1.87	46.10	0.00	14.25	8.91	9.20	21.53	0.785	0.701	22.97	12.64	9	0.1	8.75	**2.93**
DAF-84	0.5	46.20	0.00	14.45	8.62	9.27	21.45	0.786	0.701	22.92	18.45	8	0.09	14.45	**3.02**
DAFS-5	1.42	66.77	0.00	7.68	9.09	4.95	11.52	0.877	0.273	22.17	9.5	8	0.25	8.98	−0.39
DAFS-77	1.44	66.77	0.00	7.68	9.09	4.95	11.52	0.877	0.273	22.17	23.51	8	0.31	22.86	−0.27
DAFS-78	1.44	66.77	0.00	7.68	9.09	4.95	11.52	0.877	0.273	22.17	23.25	12	0.21	22.52	−0.2
DAFOL20-77	2.11	45.67	0.00	12.65	7.95	15.06	18.67	0.772	0.942	22.62	26.26	8	0.08	22.34	**2.91**
DAFOL20-84	0.54	45.69	0.00	12.65	7.91	15.13	18.63	0.772	0.945	22.61	18.09	8	0.18	14.35	**2.77**
DAFT30-67	1.6	31.26	29.21	9.67	8.88	6.27	14.71	0.736	0.436	24.31	18.68	8	0.15	12.82	**4.86**
DAFT30-5	1.6	31.39	28.99	9.70	8.90	6.29	14.72	0.736	0.436	24.3	14.1	8	0.07	8.45	**4.68**
DAFST25-78	1.2	48.92	24.92	5.47	8.84	3.44	8.41	0.818	0.177	23.5	24.05	8	0.08	22.75	**0.36**
DAFST25-5	1.2	48.93	24.92	5.46	8.81	3.48	8.40	0.818	0.179	23.5	10.32	6	0.15	8.56	**0.83**
DAF20-67	2.34	41.37	0.00	13.00	17.88	8.29	19.46	0.761	0.504	23.93	17.76	5	0.18	13.12	**3.66**
HAFC11-5	1.47	49.54	0.00	14.17	8.95	16.38	10.95	0.803	0.653	22.14	24.78	12	0.17	22.56	**1.26**
HAFC16-5	1.79	46.04	0.00	13.24	9.12	15.15	16.45	0.779	0.826	22.59	25.84	7	0.09	22.06	**2.78**
HAFS-5	0.89	64.37	0.00	12.31	9.10	14.22	0.00	0.878	0.234	21.28	21.36	7	0.07	23.25	−2.76
DAFST15-78	1.28	56.94	14.46	6.32	8.52	4.07	9.68	0.846	0.222	22.89	24.04	8	0.09	22.65	**0.45**
HAFC16S-5	1.31	60.50	0.00	9.04	8.95	10.35	11.15	0.846	0.466	22.13	24.08	7	0.12	22.65	**0.48**
DAFSM13-77	1.39	60.79	0.00	6.92	9.12	12.94	10.23	0.839	0.584	22.08	24.1	7	0.12	22.54	**0.61**
DAF5-67	1.66	48.28	0.00	15.09	4.25	9.66	22.73	0.796	0.807	22.47	16.82	8	0.12	12.71	**3.14**
DA/DAFT10-78	1.83	45.74	5.29	14.33	4.76	9.15	20.74	0.79	0.720	22.72	26.6	4	0.03	22.17	**3.41**
DAFT10-67	1.75	41.61	9.48	12.75	8.63	8.26	19.27	0.771	0.616	23.36	18.33	5	0.1	12.91	**4.43**
HRF20-29	1.8	52.27	0.00	10.30	17.53	9.69	10.21	0.815	0.303	23.15	24.71	10	0.09	22.62	**1.13**
HAF-4	0.79	56.13	0.00	16.16	9.09	18.62	0.00	0.847	0.349	21.3	20.46	8	0.98	20.66	−1.1
SAF-42	0.94	65.29	0.00	16.67	8.85	0.00	9.18	0.906	0.000	21.98	12.82	8	0.64	14.47	−2.54

I-^{18}O index calculated according the Zhao and Zheng (2003); NBO/T ratio calculated according to Mysen and Richet (2005), all Fe^{3+} assumed as a network-former and all Fe^{2+} as a nework-modifier; M.A.M. – mean atomic mass; $\delta^{18}O$ SIMS – the $\delta^{18}O$ V-SMOW values derived with normalization to the NIST 610 ($\delta^{18}O_{V-SMOW}$ = 10.9‰, Kasemann et al. (2001)); $\delta^{18}O$ LF – laser fluorination data reported in V-SMOW scale. The 1σ values are the external reproducibility of $\delta^{18}O$ on each material.

summarized in Table 2.

2.2. Electron microprobe analyses

The composition of the various SAFCMT glasses (Table 1) were determined with a Cameca SX100 electron microprobe (Institut für Mineralogie, Leibniz Universität Hannover, Germany), using a 15 keV accelerating voltage, 15 nA beam current, 10–20 s counting time, a focused beam, and employing natural and synthetic minerals and glasses as calibrants. At least ten points were analyzed on each glass sample and the results were averaged. No significant compositional variations were observed between chips of the same material.

2.3. Laser fluorination analysis

Laser fluorination gas source mass spectrometry (LF GS-MS) oxygen isotope ratio determinations were conducted both on this suite of SAFCMT and on the three MPI-DING glasses at the IGEM RAS, Moscow

Table 2

Chemical (wt%) and oxygen isotope composition of glasses used as standard with SIMS measurements.

Sample	Short description	Glass composition (wt%)										Total
		SiO_2	TiO_2	Al_2O_3	FeO_t	MgO	CaO	Na_2O	K_2O	MnO	P_2O_5	
ATHO-G[a]	rhyolite	75.6	0.26	12.2	3.27	0.1	1.7	3.75	2.64	0.11	0.03	99.65
StHs6/80-G[a]	andesite	63.7	0.7	17.8	4.37	1.97	5.28	4.44	1.29	0.08	0.16	99.79
KL2-G[a]	basalt	50.3	2.56	13.3	10.7	7.34	10.9	2.35	0.48	0.17	0.23	98.33
NIST 610[b]	synthetic glass	68.89	0	1.91	0	0	11.34	13.88	0	0	0	96.02

Sample	Composition-dependent parameters			Oxygen isotope data (*)					IMF
	I-^{18}O	NBO/T	M.A.M.	$\delta^{18}O$ SIMS, ‰ drift-corrected	n	1σ	$\delta^{18}O$ LF(A), ‰	$\delta^{18}O$ LF(B), ‰	
ATHO-G	0.938	0.065	21.090	0.58	8	0.12	3.33	3.2	−3.76
StHs6/80-G	0.899	0.163	21.449	5.78	6	0.15	6.16	6.12	−1.34
KL2-G	0.824	0.777	22.973	11.32	8	1.01	9.16	8.63	1.23
NIST 610	0.871	0.688	21.071	10.91	29	0.14	nd	10.91	−0.91

I-^{18}O index calculated according the Zhao and Zheng (2003); NBO/T ratio calculated according to Mysen and Richet (2005), all Fe^{3+} assumed as a network-former and all Fe^{2+} as a nework-modifier; M.A.M. – mean atomic mass; $\delta^{18}O$ SIMS – the $\delta^{18}O$ V-SMOW values derived with normalization to the NIST 610 ($\delta^{18}O_{V-SMOW}$ = 10.9‰, Kasemann et al. (2001)); $\delta^{18}O$ LF – laser fluorination data reported in V-SMOW scale: $\delta^{18}O$ LF(A) – the values measured in this work, $\delta^{18}O$ LF(B) – published data (Jochum et al., 2006; Kasemann et al., 2001). The 1σ values are the external reproducibility of $\delta^{18}O$ on each material.

[a] Chemical composition are from Jochum et al. (2006).
[b] Chemical composition from Hinton (1999).

(for details see Dubinina and Borisov, 2018). Following the procedure of Valley et al. (1995) the data were calibrated on the V-SMOW scale using quartz NBS-28 ($\delta^{18}O = 9.57 \pm 0.10$‰, Dargie et al., 2007) and garnet UWG-2 ($\delta^{18}O = 5.80 \pm 0.06$‰, Valley et al., 1995). The $\delta^{18}O_{V\text{-}SMOW}$ values 5.16 ± 0.10‰ and 5.27 ± 0.10‰ (1σ) were obtained for the two-quality control materials biotite NBS-30 ($n = 8$, recommended value of 5.12 ± 0.06‰, Dargie et al., 2007) and San Carlos olivine ($n = 18$, published values ranges from 4.98‰ (Franchi et al., 1999) to 5.44‰ (Kusakabe et al., 2004)), respectively. We estimate the total uncertainty of our $\delta^{18}O$ measurements at $\leq \pm 0.10$‰ (1σ). For some high-silica glasses the RM bracketing technique was applied with the repeatability of $\delta^{18}O$ values equal to ±0.15‰ (Dubinina and Borisov, 2018). Our measurements were done with the isotopic ratio mass-spectrometer (IRMS) DeltaPlus (Thermo, Germany) using dual-inlet mode employing as a reference the high-purity, commercially available O_2 gas (in-house O_2-IGEM reference gas) calibrated with respect to V-SMOW by E. Barkan at the Hebrew University of Jerusalem (assigned $\delta^{18}O$ value is $+34.99$‰). The oxygen isotope compositions determined by GS-MS with laser fluorination of the SAFCMT and MPI-DING glasses, expressed on the V-SMOW scale, are reported on Tables 1 and 2, respectively.

2.4. SIMS analysis

We used the Cameca 1280-HR instrument at the GFZ Potsdam to determine oxygen isotope ratios in 27 SAFCMT synthetic glasses and three MPI-DING glasses with natural compositions. Chips of all of these materials were cast in a single 1-in. diameter, round epoxy mount that had a topographic flatness of better than 10 μm – gas bubbles exposed during polishing were filled with epoxy as best as possible and areas near locations with poor topographic contact between the epoxy matrix and the glass samples were avoided for the analyses. Prior to analysis the sample mount was cleaned in a high-purity ethanol ultrasonic bath and then coated with a 35 nm thick high-purity gold coat to assure electrical conductivity.

These $\delta^{18}O$ determinations employed a ~ 2 nA $^{133}Cs^+$ beam focused to a ~ 5 μm diameter on the polished sample surface. The total impact energy of the Cs^+ ions was 20 keV. Each analysis was preceded by a 2 nA, 20×20 μm rastered pre-sputter for 90 s. Charge compensation was achieved with low-energy, normal incidence electron flooding using a ~ 1.0 μA current, or approximately 500 times larger than our $^{133}Cs^+$ primary current. In order to suppress within-run drift in the isotope ratio, a 10×10 μm raster was employed during data collection, thereby producing a flat-bottom crater geometry. The rastering of the primary beam during data collection was compensated by using the dynamic transfer capability of our secondary column's ion optics. All analyses were conducted within the innermost 16 mm of the round sample mount.

Secondary ions were accelerated by a -10 kV potential applied to the sample holder. Prior to the start of data acquisition, the 1280-HR conducted automated centering routines for the field aperture in both X and Y as well as in X direction on the contrast aperture. We employed an 80×80 μm field of view in conjunction with a 50 V energy band-pass, but with no energy offset applied. The mass spectrometer was operated in static multi-collection mode, with the $^{16}O^-$ being collected in the L2' Faraday cup and the $^{18}O^-$ signal being collected in the H2' Faraday cup; the amplifier system employed thermally stabilized 10^{10} Ω and 10^{11} Ω amplifiers, respectively. Magnetic field drift on the mass spectrometer was effectively eliminated by the use of a NMR-controlled feedback loop. The mass resolution of the instrument was set at $M/\Delta M \approx 1900$, which is effectively full transmission of the instrument and which is sufficient to discriminate both the $^{16}O^1H_2$ and the $^{16}O^2H$ isobaric interferences from the ^{18}O mass station. A single analysis consisted of 20 integrations of 4 s each, resulting in a total data collection time of 80 s per analysis, equivalent to ~3 min per point when including the pre-sputter and automatic beam centering routines. This analytical design resulted in a count rate of $\sim 2 \times 10^9$ $^{16}O^-$ ions per second on the NIST

610 glass. A total of 271 analyses were determined on the various glass materials along with an additional 31 analyses on the NIST 610 silicate glass RM. Data collection was run in fully automated mode and a 3σ filter was applied with respect to the 20 quasi-independent integrations acquired during each analysis. The list of analyses in chronological order is provided in Table A of the electronic annex.

Data were evaluated for the presence of a time dependent drift by using the interspersed analyses of the NIST 610 glass to correct for a 0.3‰ total drift over the 18 h of entire analytical routine (Table A1 of the electronic annex). The 31 drift-corrected determinations of $^{18}O^-/^{16}O^-$ conducted on NIST 610 yielded an analytical repeatability of 0.14‰ (1σ). Apparent (i.e., not corrected for the matrix effect) $\delta^{18}O$ compositions of the unknowns were derived by normalizing their measured $^{18}O/^{16}O$ ratios to the NIST 610 reference material, using an absolute value of $^{18}O/^{16}O = 0.0020271$ for NIST 610 as derived from the $\delta^{18}O_{SMOW} = 10.9$ value reported in Kasemann et al. (2001) and absolute zero-point of $(^{18}O/^{16}O)_{SMOW} = 0.00200520$ (Baertschi, 1976). These NIST 610 analyses gave a measured/true value $= 0.99908$ indicating an overall IMF of -0.91‰ for the NIST 610 silicate glass. All $^{18}O/^{16}O$ isotope ratios measured and IMF calculations are summarized in Table B of the electronic annex.

3. Results

3.1. SAFCMT glasses

The suite of 27 synthetic SAFCMT glasses was analyzed by both laser fluorination in IGEM RAS (Moscow) and using the Potsdam Cameca 1280-HR, allowing us to calculate an individual IMF value for each of these materials. Chemical major element compositions and bulk laser fluorination determined oxygen isotope compositions for these glasses are reported in Table 1, which also includes drift-corrected $\delta^{18}O$ values obtained by the 1280-HR based on the NIST 610 calibration. Additionally, the calculated atomic masses of SAFCMT glasses and indices NBO/T (the ratio of number of non-bridging oxygen atoms to tetrahedrally coordinated cation, calculated according to Mysen and Richet, 2005) are also presented in the Table 1. The results show significant variations in IMF ranging from $+4.86$ to -2.76‰ (Table 1). True $\delta^{18}O$ values obtained for these glasses using laser fluorination technique vary from 8.45 to 23.25‰ while the $\delta^{18}O$ (NIST 610) values determined using the Potsdam SIMS instrument range from 9.50 to 26.60‰. For the majority of these 27 materials the $\delta^{18}O_{SIMS}$ values are higher than the "true" $\delta^{18}O$ as determined by laser fluorination (Table 1). Nearly all of the 27 SAFCMT glasses had internal repeatability similar to the repeatability seen on NIST 610 glass (± 0.14‰, 1σ, $n = 29$) after correcting for the small amount of drift that occurred, indicating that no significant isotope ratio heterogeneity is present within individual SAFCMT glasses. Exception are only the two samples HAF-4 and SAF-42 that had low SIMS repeatability ±0.98 and ±0.64‰, 1σ, respectively (Table 1).

Our data show that shifts in the various oxide contents induce significant changes in sputtering behavior. Pair correlations (R^2, standard

Table 3
Correlation of the IMF values detected in SAFCMT glasses with molar part of single oxide and composition-dependent parameters.

Parameter	R^2	Slope	Intersection	1σ
SiO_2	0.82	-18.97	11.54	0.90
TiO_2	0.07	6.94	1.38	2.03
Al_2O_3	0.05	22.54	0.10	2.05
FeO_t	0.02	-8.53	2.29	2.09
MgO	0.02	4.15	1.09	2.09
CaO	0.66	23.74	-2.07	1.22
Fe^{3+}/Fe^{2+}	0.25	2.30	-1.75	1.87
NBO/T	0.46	5.13	-1.01	1.55
Mean Atomic Mass	0.43	1.75	-38.02	1.57
I-^{18}O	0.87	-42.67	36.32	0.75

error, slope and intersects of linear equations) were calculated between the IMF value and molar part of each oxide in glasses (Table 3). Only two of the six oxides (SiO_2 and CaO) show a meaningful correlation, with R^2 equal to 0.82 and 0.66, respectively. These data show that IMF is strongly anticorrelated with SiO_2 content, namely $IMF = -0.19[SiO_2] + 11.54$, where $[SiO_2]$ is in mole percent (Fig. 1). However, despite a high R^2 value of 0.82 for this system, the overall distribution of residuals remains high ($1\sigma = 0.90‰$). It should be noted that two samples fall well off the best-fit correlation line, both of which are Ca-free. The slope of linear relationship between the IMF and $[SiO_2]$ is -0.19 and corresponds to a 0.2‰ increase in bias towards lower $\delta^{18}O$ values with the addition of every one mole percent of SiO_2. The IMF values derived in reference MPI-DING glasses also correlate with their SiO_2 contents. We note that the high-Na reference glass NIST 610 falls slightly outside the 1σ confidence level. The CaO content showed some influence on the IMF, but this correlation ($R^2 = 0.63$, Table 3) is much weaker than is the case for silica.

Some of our SAFCMT glasses were synthesized from identical chemical mixtures that were then melted under differing experimental conditions (i.e., flushing the furnace with different gases, using different temperature regimes etc.) resulting in differing oxygen isotope compositions. Thus, three pairs of glasses (with the compositions DAFST25, DAFOL20 and DAFT30, Table 1) and two triplets (with the compositions DAF and DAFS, Table 1) have identical chemical compositions but significantly differing in O-isotope compositions (see Table 1). Within each pair or triplet, the IMF is constant (Fig. 2). The fact that these glasses with the same chemical composition have the same values for their IMF despite differing oxygen isotope compositions demonstrates that chemical composition alone is the controlling factor for defining IMF values in SAFCMT glasses. This test shows, as expected, that IMF value is not dependent on the true $\delta^{18}O$ values of glasses, which is to say the chemical matrix effect is not meaningfully influenced by a material's oxygen isotope ratio.

3.2. Alkali-bearing reference glasses

The oxygen isotope ratios of three MPI-DING glasses with natural compositions from basalt to rhyolite (ATHO-G, KL2-G and StHs6/80-G, Jochum et al., 2006) were analyzed by both laser fluorination GS-MS and the Cameca 1280-HR SIMS (Table 2). Our GS-MS laser
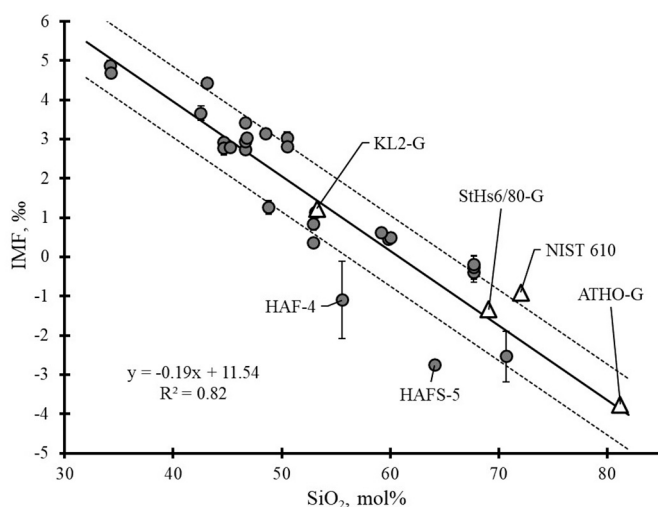

Fig. 1. IMF determined for the SAFCMT experimental glasses vs. their SiO_2 content.
Best-fit correlation line (solid) derived for the 27 SAFCMT glasses, dashed lines are the $1\sigma = \pm 0.90‰$ interval. Triangles denotes the data derived in reference MPI-DING and NIST 610 glasses. Points HAF 4 and HAFS-5 are the samples with Ca-free chemical composition (Table 1).
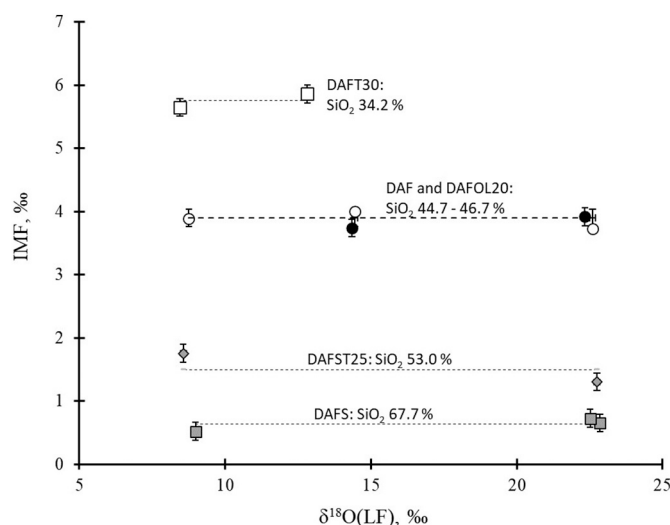

Fig. 2. The IMF value in five groups of the experimental SAFCMT glasses. Each group of the glasses (DAFS, DAFST25, DAF, DAFOL20 and DAFT30) consists of 2 or 3 sample with the same chemical composition but with different $\delta^{18}O(LF)$ values. Dashed lines are the averages for each group, error bars for SIMS are $\pm 0.14‰$ and for LF is $\pm 0.1‰$.

fluorination data of MPI-DING glasses point to some variability in the oxygen isotope composition of the KL2-G basalt glass. The $\delta^{18}O$ value of KL2-G measured by us using laser fluorination is $9.16 \pm 0.18‰$ ($n = 3$), whereas the published value is significantly lower ($8.63 \pm 0.09‰$, Jochum et al., 2006). A similar degree of $\delta^{18}O$ heterogeneity for KL2-G was detected earlier (Ickert et al., 2008) during SHRIMP II analyses. During our SIMS analytical session, the KL2-G glass also had poor repeatability ($\pm 1.01‰$, 1σ, Table 2), indicating that significant isotope ratio heterogeneity is present within this reference sample. Hence, the variable $\delta^{18}O$ results for KL2-G suggest this particular glass is not sufficiently homogeneous to use for precise calibration of SIMS O-isotope data. Our calculations employing KL2-G for calibrating our 1280-HR data are based on our LF GS-MS VSMOW value of 9.16, as both the LF and SIMS analyses used glass chips produced from a single fragment of the KL2-G glass.

The $\delta^{18}O$ values obtained by GS-MS for the other two MPI-DING glasses ATHO-G and StHs6/80-G are very similar to the values published by Jochum et al. (2006) (Table 2). The three MPI-DING glasses showed a strong linear correlation ($R^2 = 0.99$) between IMF and SiO_2 content (Fig. 3). The IMF measured for these glasses ranged from $+1.2$ to $-3.8‰$ while the SiO_2 concentrations span from 53.4 to 81.3 mol% (see Table 2). Similar correlations for these MPI-DING glasses have been previously reported for both Cameca 1270 (Hartley et al., 2012) and SHRIMP II (Ickert et al., 2008) instruments. Despite the consistent data pattern obtained using multiple instrument types the slopes of the correlation lines in Fig. 3 are nearly the same.

4. Discussion

The nature of the chemical effect on the IMF in silicate glass matrices can be influenced by the physical (density, molar volume, atomic mass, etc.), structural (polymerization) and energy (mean Metal-O bond energy) properties of the given glass matrix. The data presented here allow us to consider all these parameters due to the variable chemistry of the SAFCMT glasses. This suite of materials varies in chemical compositions from haplo-basalt to haplo-rhyolite (SiO_2 from 31.3 to 66.8 wt%). Compared to natural glasses, they contain oxides covering a much broad compositional range: TiO_2 from 5.3 to 29.2, Al_2O_3 from 5.5 to 16.7, MgO from 3.4 to 18.6, CaO from 8.4 to 23.6 and total FeO from 4.3 to 17.9 wt %. The observed SIMS IMF values for these glasses also vary over a broad
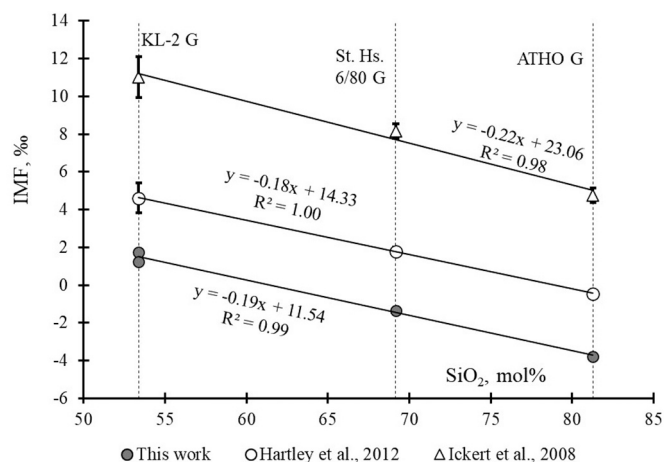
Fig. 3. The IMF values obtained for standard MPI-DING glasses basalt KL2-G, andesite StHs6/80-G and rhyolite ATHO-G vs theirs SiO_2 content. Dashed lines correspond to each glass reference material. Two points for the glass KL2-G were obtained by calculation of IMF using published $\delta^{18}O$ laser fluorination data (Jochum et al., 2006) and using the laser fluorination data obtained in this present work.

range from -2.76 to $+4.86‰$. With this nearly 8‰ range, geochemically meaningful data can only be achieved with a robust correction algorithm. Since all data were obtained during a single, fully-automated session with the 1280-HR instrument, variations in instrumental tuning cannot play a role in our dataset. Likewise, our samples being glasses, crystallographic orientation can be excluded from our discussion. Thus, only variations in the chemical composition of glasses can be responsible for IMF variations between the SAFCMT glasses. It is important that SAFCMT glass suite is free of trace elements, so this topic can also be excluded from consideration.

Several earlier studies have addressed IMF corrections applied to silicate glass matrices. Most correction models have been based on single or combined oxide concentrations (e.g., Hartley et al., 2012; Gurenko et al., 2001; Gurenko and Chaussidon, 2002). Hartley et al. (2012) also investigated other parameters such as molar volume, mean cation mass and liquidus density, but these parameters were found unsuitable for SIMS data correction. The mean atomic mass and the average atomic masses of network former and network modifier cations were also studied by Eiler et al. (1997). However, these parameters were only partially successful for predicting IMF.

Here we considered both the effects of single oxides (SiO_2, Al_2O_3, FeO, CaO, MgO, TiO_2) and the potential applicability of composition-dependent parameters: mean atomic mass and NBO/T ratio (Table 1) for correcting the IMF for the 27 SAFCMT glasses. The resulting correction equations were assessed using 4 reference glasses: rhyolite ATHO-G, andesite StHs6/80-G, basalt KL2-G and the sodium-rich NIST 610.

4.1. Effects of atomic mass and NBO/T ratio on IMF values

The influence of mean atomic mass (MAM) on O-isotope IMF value was first discussed by Eiler et al. (1997) who studied both silicate minerals and glasses with natural chemical compositions; they found that the IMF for both mineral and glass analyses was positively correlated with this parameter. Indeed, our data from the SAFCMT glasses confirm that a positive correlation exists between IMF and MAM (Table 1), but it is not sufficiently robust to produce geologically meaningful results ($R^2 = 0.45$, Table 3).

If IMF is predominantly structure dependent, a strong correlation should exist between the IMF and the ratio of non-bridging oxygens per tetrahedrally coordinated cation, NBO/T, because the last reflects the

extent of polymerization of a silicate glass (Mysen and Richet, 2005). Despite observing that IMF increases with increasing NBO/T ratio, the correlation with this parameter is also poor ($R^2 = 0.46$, Table 3). We note that using a simple correction based only on silica contents results in a much stronger correlation with $R^2 = 0.82$ (see Fig. 1). Our data confirm that neither mean atomic mass nor NBO/T ratio alone are adequate for modeling IMF in silicate glasses.

4.2. Effects of single oxide contents on IMF values of silicate glasses

SiO_2 content is the single most important parameter influencing oxygen isotope IMF in silicate glasses. The large influence of SiO_2 on IMF is demonstrated both for the SAFCMT (Fig. 1, Table 3) and the MPI-DING glasses (Fig. 3). In general, as silica content increases SIMS results trend towards lower $^{18}O/^{16}O$ measured by SIMS relative to the "true" isotope composition defined by laser fluorination. This strong negative correlation between IMF and SiO_2 wt% in silica glasses has been discussed previously by Gurenko et al. (2001), Gurenko and Chaussidon (2002), Ickert et al. (2008) and Hartley et al. (2012). We too have also observed this strong negative correlation of IMF with SiO_2. We note that the correlation between the SiO_2 content and IMF is slightly better when based on mole percent used for calculations, as opposed to using wt%: for the 27 SAFCMT glasses we calculate a R^2 value of 0.78 based on SiO_2 (wt%) whereas a R^2 value of 0.82 when using SiO_2 (mol %).

The -0.19 slope of the linear trend defined by our data (Fig. 3) is intermediate to the slopes for published data of -0.18 and -0.22 reported by Hartley et al. (2012) and Ickert et al. (2008), respectively. A very similar regression line slope for IMF versus wt% SiO_2 was derived for basaltic and andesitic in-house reference glasses (-0.197, Gurenko and Chaussidon, 2002). Furthermore, we note that these slope values are similar to the slope we observed on our SAFCMT synthetic glasses (-0.19, see Table 3). Thus, a shift in instrumental bias of circa $-0.2‰$ for every 1 mol% increase in SiO_2 contents is common to all these studies and is applicable to both Cameca and SHRIMP instruments. We calculated the empirical relation of IMF with the mole fraction of SiO_2 in 27 SAFCMT glasses in the linear form:

$$IMF = -18.97X_{SiO2} + 11.54 \qquad (2)$$

Statistical data for Eq. (2) are given in Table 4 and the calculated IMF values derived from Eq. (2) are provided in Table C of the electronic annex.

Despite the good correlation of the IMF value with SiO_2 contents, this approach alone does not fully address the challenges of the chemical matrix effect. For example, the glasses of DAFS and DAFST25 compositions show similar IMF values close to zero, although their silica contents differ substantially (66.7 and 49.0 mol% SiO_2, respectively). A similar conclusion is also true for DA, DAF and DAFOL20 samples. These haplo-basalt glasses have a range of SiO_2 contents from 45 to 50 mol%, but their IMF values are essentially identical ($2.93 \pm 0.12‰$). The high-Na NIST 610 glass and Ca-free HAF and HAFS glasses scatter on Fig. 1, confirming that SiO_2 contents alone does not define IMF value. In general, the materials that are extremely enriched in other metal oxides (TiO_2, MgO, etc. see Table 1) diverge most from the SiO_2 – IMF trend.

With the exception of SiO_2, CaO is the only other species showing significant influence on IMF (Table 3). For CaO we observed a positive correlation with IMF ($R^2 = 0.63$). The slope of the regression line derived for CaO content (Table 3) shows an effect of circa 0.3‰ of IMF for each mol% of CaO. These results confirm the observations about SiO_2 and CaO reported by Hartley et al. (2012). In contrast, compared to the data of Hartley et al. (2012) we did not find any significant correlations of IMF with the other oxides contained in our SAFCMT glasses (TiO_2, Al_2O_3, MgO and FeO) (Table 3). It is noteworthy that strong negative correlations with SiO_2 and positive correlations with CaO contents were reported by both Eiler et al. (1997) and Gurenko et al. (2001).

Table 4

Equations for the IMF prediction based on the chemical composition (mole part of major oxides) and I-^{18}O index of silicate glasses.

Equation based on:	Eqn. No	n	Equation	R^2	Standard error (1σ, ‰)
Single SiO$_2$ in SAFCMT glasses	(2)	27	IMF = [−18.97 ± 1.81]·(X$_{SiO2}$) + [11.54 ± 0.95]	0.82	0.90
Multivariant 6 oxide contains in SAFCMT glasses	(3)	27	IMF = [−6.16 ± 0.49]·(X$_{SiO2}$) − [9.70 ± 4.69]·(X$_{Al2O3}$) + [7.52 ± 1.03]·(X$_{TiO2}$) + + [8.07 ± 1.31]·(X$_{MgO}$) + [22.50 ± 1.23]·(X$_{CaO}$) + [7.90 ± 2.45]·(X$_{FeOt}$)	0.98	0.40
I-^{18}O index of SAFCMT glasses	(7)	27	IMF = [−42.67 ± 3.24]·(I-^{18}O) + [36.32 ± 2.63]	0.87	0.75
Multivariant 8 oxides contained in SAFCMT glasses and four reference glasses	(8)	31	IMF = [−6.44 ± 0.50] ·(X$_{SiO2}$) + [21.50 ± 1.24] · (X$_{CaO}$) + [−3.97 ± 4.30] · (X$_{Al2O3}$) + +[7.61 ± 1.10] · (X$_{TiO2}$) + [8.28 ± 2.54] ·(X$_{FeOt}$) + [7.25 ± 1.35]· (X$_{MgO}$) + + [61.79 ± 31.61]·(X$_{K2O}$) + [8.49 ± 3.84]· (X$_{Na2O}$)	0.98	0.43

4.3. Estimation of IMF values based on multivariant oxide contents

We calculated best-fit empirical equation involving the correlation with all six oxides in our 27 SAFCMT glasses using multiple linear regression in the form IMF = $\sum d_i X_i$ + C, where d_i is the empirical coefficient and X$_i$ is the molar value of oxide i:

$$IMF = -6.16X_{SiO2} - 9.70X_{Al2O3} + 7.52X_{TiO2} + 8.07X_{MgO} + 22.50X_{CaO} + 7.90X_{FeOt} \quad (3)$$

The constant C in Eq. (3) was set to be zero. Corresponding statistical data for this equation is given in Table 4. Eq. (3) in Table 4 returns IMF values with standard error of 0.4‰, which is better than the standard error of 0.9 permil in Eq. (2) when X_{SiO2} is used as the only parameter. The calculated IMF values with Eq. (3) are provided in Table C of the electronic annex.

Eq. (3) provides a reliable estimate for predicting the SIMS oxygen isotope IMF in alkali-free glasses with SiO$_2$-Al$_2$O$_3$-FeO$_t$-CaO-MgO-TiO$_2$ compositions. The empirical coefficients d_i in (3) vary from minimal values of −9.70 and − 6.16 for Al$_2$O$_3$ and SiO$_2$, respectively, to a maximal value of +22.50 for CaO. One can see that minimal d_i values correspond to cations with small ionic radii (Al and Si) and the maximal d_i value corresponds to Ca which has a large ionic radius. In Fig. 4 we plot the values of d_i from Eq. (3) vs. ionic radii of the corresponding cations, r_{ct} (cation radii are taken from Shannon, 1976). For Si and Al, we took the r_{ct} values for cations in IV coordination, for all other cations in VI coordination. Since the Fe^{3+}/Fe^{2+} ratio in our experimental glasses varies from 0.5 to 2.3 (see Table 1) the mean r_{ct} value of Fe^{2+} and Fe^{3+} was used. The resulting best-fit equation (R^2 = 0.92, Fig. 5) clearly demonstrates that small cations (e.g., Si^{4+} and Al^{3+}) are associated with negative d_i values whereas large cations (e.g., Ca^{2+}) have the highest positive coefficients in Eq. (3). The ions Ti^{4+}, Fe$^{2+/3+}$ and Mg^{2+} all have intermediate positive coefficients that are very similar to each other.
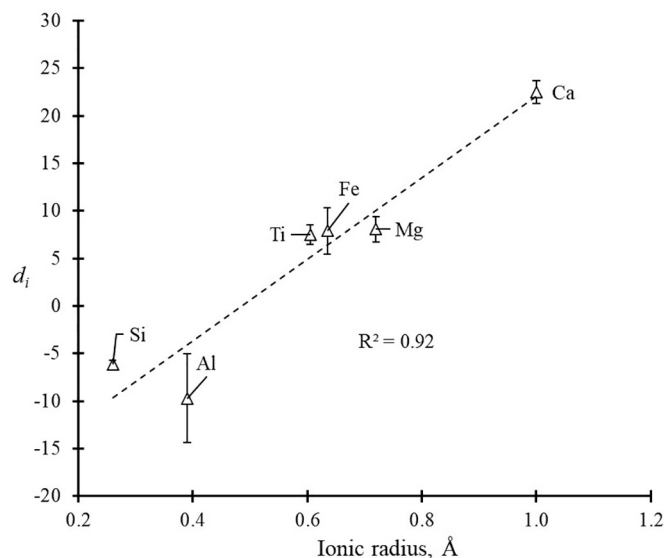

Fig. 4. The empirical coefficients d_i from the Eq. (3) vs ionic radii of cations. Uncertainty estimates corresponds the 1σ for Eq. (3). The values of r_{ct} used according the Shannon (1976). For Si^{4+} and Al^{3+} the IV coordination and for other cations the VI coordination was accepted. For Fe$^{2+/3+}$ the mean value of r_{ct} of Fe^{3+} and Fe^{2+} was used (see text for details).
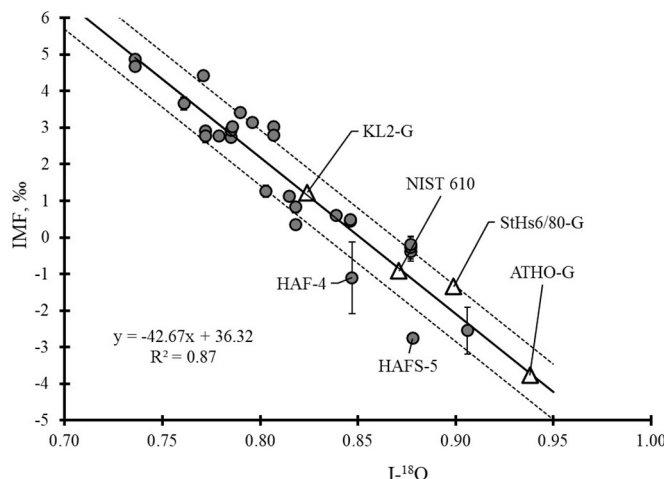

Fig. 5. The IMF SIMS values of experimental SAFCMT and standard glasses vs I-^{18}O index.

Correlation line (solid) derived for the 27 experimental SAFCMT glasses, dashed lines restrict the 1σ (± 0.75‰, Table 3) interval. Triangles denotes the data derived from reference glasses with natural compositions. Points HAF 4 and HAFS-5 are the samples with Ca-free chemical composition.

4.4. Estimating IMF using isotope I-^{18}O index

The strong correlation obtained in Fig. 4 substantiates our hypothesis that cation-oxygen bond strength is a core determinant of SIMS IMF. To illustrate this, we can use the isotope I-^{18}O index which was originally proposed by Schütze (1980) for describing the observed correlation between atomic bond strength and relative oxygen isotope enrichment in silicate minerals. This index has been used for investigating the ^{18}O-enrichment of oxides, minerals and rocks (Hoffbauer et al., 1994; Zheng, 1991, 1993, 1999). According to Hoffbauer et al. (1994) the I-^{18}O index takes into account the bonding strength of each element (i_{c-O}) compare

to silicon bonding strength (i_{Si-O}) in a mineral divided by the number of oxygen bonds (n_0):

$$I\text{-}^{18}O = \frac{\left[\sum \left(\frac{i_{c-o}}{i_{Si-O}} \right) V_c n_c F \right]}{2n_0} \quad (4)$$

In turn, the bonding strength depends on the valence of the given cation (V), its coordination number (CN), the cation mass (m_c) and the corresponding ionic radius (r_c, r_O):

$$i_{c-O} = \frac{V_c}{(r_O + r_c)} CN \cdot \left[\sqrt{\frac{(m_c + 16)18}{(m_c + 18)16}} - 1 \right] \quad (5)$$

For silicate glasses the I-^{18}O index for the major element oxides can be used to calculate the I-^{18}O index of each glass sample, as has been previously applied to bulk silicate rock compositions (Zhao and Zheng, 2003):

$$I\text{-}^{18}O(glass) = \sum X_{oxide} \cdot I\text{-}^{18}O(oxide) \quad (6)$$

where X_{oxide} is the molar concentration of the oxide in the silicate glass. For the purpose of calculating the I-^{18}O indices for the SAFCMT and MPI-DING glasses in Tables 1 and 2 we used the revised values of I-^{18}O indices for major element oxides from Zhao and Zheng (2003). The best-fit linear equation based on the I-^{18}O index has the form:

$$IMF = -42.67 \left(I\text{-}^{18}O \right) + 36.32 \quad (7)$$

Statistical data for Eq. (7) are given in Table 4, the calculated IMF values based on this equation are provided in Table C of the electronic annex.

The IMF values of both the SAFCMT and the MPI-DING glasses demonstrate a strong linear correlation with I-^{18}O indices (Fig. 5). This correlation is better ($R^2 = 0.87$) than is the case using SiO_2 contents in mol% alone ($R^2 = 0.82$, Fig. 1). The standard error of the approximation with I-^{18}O index ($1\sigma = 0.75‰$) is less than the standard error of the approximation with the X_{SiO2} in silicate glasses ($1\sigma = 0.90‰$). We conclude that the I-^{18}O index better predicts IMF values for silicate glasses than does using SiO_2 content alone. This approach predicts well the IMF of both the SiO_2-rich ATHO-G glass as well as the andesite glass StHs6/80-G, which was poorly modeled by both the bivariant and multivariant oxide correction models of Hartley et al. (2012).

A correlation of IMF value with I-^{18}O index was assessed based on the 27 SAFCMT glasses which contain only six major oxides (SiO_2, Al_2O_3, FeO_t, CaO, MgO and TiO_2) while this index for our other four materials (MPI-DING and NIST 610) was calculated using a suite of 10 major oxides (i.e. Na_2O, K_2O, MnO and P_2O_5 were additionally included). From these observations we conclude that the I-^{18}O index is a more robust approach for predicting the IMF as compared to previously existing strategies. At the moment we recommend Eq. (7) based on the I-^{18}O index which can predict the IMF with a standard error of $\pm 0.75‰$ (1σ), which is approaching the data quality needed by for many geochemical applications.

The dependence the coefficient d_i on the r_{ct} (Fig. 5) is consistent with the strong correlation obtained between IMF and the I-^{18}O index in SAFCMT glasses; according to Eqs. (4) and (5) the I-^{18}O index should anti-correlate with the ionic radius of cations. Furthermore, from the relationship shown in Fig. 4 it follows that alkaline oxides with large r_{ct} (for example, K_2O, $r_{ct} = 1.46$ Å) can increase the IMF value significantly.

We went on to calculate an equation that additionally included K_2O and Na_2O oxides in the 27 SAFCMT glasses and 4 other silicate glasses (MPI-DING glasses and NIST 610) using a multiple linear regression:

$$IMF = -6.44X_{SiO2} - 3.97X_{Al2O3} + 7.61X_{TiO2} + 7.25X_{MgO} + 21.50X_{CaO}$$
$$+ 8.28X_{FeOt} + 61.79X_{K2O} + + 8.49X_{Na2O} \quad (8)$$

Again, for this calculation the equation was forced through the origin similar to how we addressed Eq. (3). This refined equation has a high R^2

value (0.98) and small standard error (0.43‰) (Table 4). Using the data shown in the Fig. 4 we can predict that the small B^{3+} and P^{5+} species (with r_{ct} equal to 0.27 and 0.38 Å, respectively) would have d_i coefficients lower than those for Si^{4+} ($r_{ct} = 0.41$ Å). Accordingly, we can expect that commercial borosilicate and phosphate glasses should have more negative IMF values than high-silica glasses. The correlation line shown in Fig. 4 predicts that elements with r_{ct} close to 0.5 Å should have little influence on IMF.

Eq. (8) takes into account the two key alkaline oxides Na_2O and K_2O, but we stress that this equation remains preliminary as only 4 alkali-bearing reference glasses were used to derive this equation. The Na_2O contents in the four alkali-bearing standard glasses (MPI-DING and NIST 610) range from 2.42 to 13.67 mol%. The K_2O contents range from only 0.04 to 1.81 mol% (Table 2). Due to the relatively narrow range in K_2O contents the uncertainty in the empirical coefficient d_i in the Eq. (8) for K_2O is quite high (Table 4). Any future studies of the roles of alkaline oxides on the IMF in silicate glasses should make use of additional experimental reference glasses providing a larger range in K_2O contents.

4.5. Testing the various correction schemes

We used the four Eqs. (2), (3), (7), and (8) presented in Table 4 to predict IMF values both for 27 SAFCMT and the four alkali-bearing reference glasses. The first three of these equations were derived solely from the SAFCMT glass data whereas Eq. (8) is derived from SIMS results obtained on the full suite of 31 materials. In Fig. 6a, b and c the IMF values predicted by Eqs. (2), (3), and (7) are compared with the true IMF values based on our laser fluorination data.

A model based on the Eq. (2) shows that SiO_2 content alone describes well glasses with "normal" natural compositions ranging from basalt to rhyolite, yielding geologically useful accuracy (in general bias $<0.3‰$) (Fig. 6a). However, the Na-rich glass NIST 610 is not described well by this equation, deviating by 1.2‰ from the true δ^{18}O value, despite the fact that it agrees to within the 2σ uncertainty (1.8‰) established by Eq. (2). In contrast, and despite the large 1σ interval implied by Eq. (2), this equation does not describe well all the 27 SAFCMT glasses. We note here that the suite of SAFCMT glasses includes two Ca-free materials (HAF-4 and HAFS-5) and these are the materials that yield SIMS results that diverge most strongly from Eq. (2) model predictions (Fig. 1).

Predictions based on Eq. (3) using all 6 major oxides in the SAFCMT glasses yielded poor results for the four alkali-bearing reference glasses (Fig. 6b) despite the low standard error obtained from this equation ($1\sigma = 0.40‰$, Table 4). The IMF values calculated with Eq. (3) for three of five alkali-bearing glasses are underestimated by 1.29 and 2.02‰ for ATHO-G and StHs6/80-G glasses, respectively.

Predictions based on I-^{18}O index with Eq. (7) describe well the alkali-bearing glasses (Fig. 6c); only the StHs6/80-G andesite glass shows a large bias of 0.7‰, but this deviation is nonetheless inside this equation's 1σ uncertainty envelope. All other glasses fit Eq. (7) model well.

For the case of Eq. (8), where eight elements are used for prediction, the result is even better: the δ^{18}O values in three standard glasses (ATHO-G, KL2-G and NIST 610) deviate from their true values within the narrow range of $\pm 0.3‰$ (Fig. 6d). Applying the same method for predicting the IMF of the andesite StHs6/80-G glass yields the bias between the true and Eq. (8) predicted IMF values +0.72‰ (see Fig. 6d). We note that the StHs6/80-G glass also was not predicted well with the FMCNK multivariant model of Hartley et al. (2012).

In order to compare the utility of Eqs. (2), (3), (7), and (8), we calculated hypothetical IMF values for glasses which correspond to some common silicate glass types using the models based on these equations. We used major oxide concentrations in rhyolite, syenite, andesite, diorite, basalt and peridotite (Table D of the electronic annex) which were used by Zhao and Zheng (2003) for I-^{18}O index calculation. Also, the IMF value for one common reference material (NIST 610) was calculated using the each of our four equations. This allowed us to calculate the bias between the IMF values of hypothetical rocks and the NIST 610
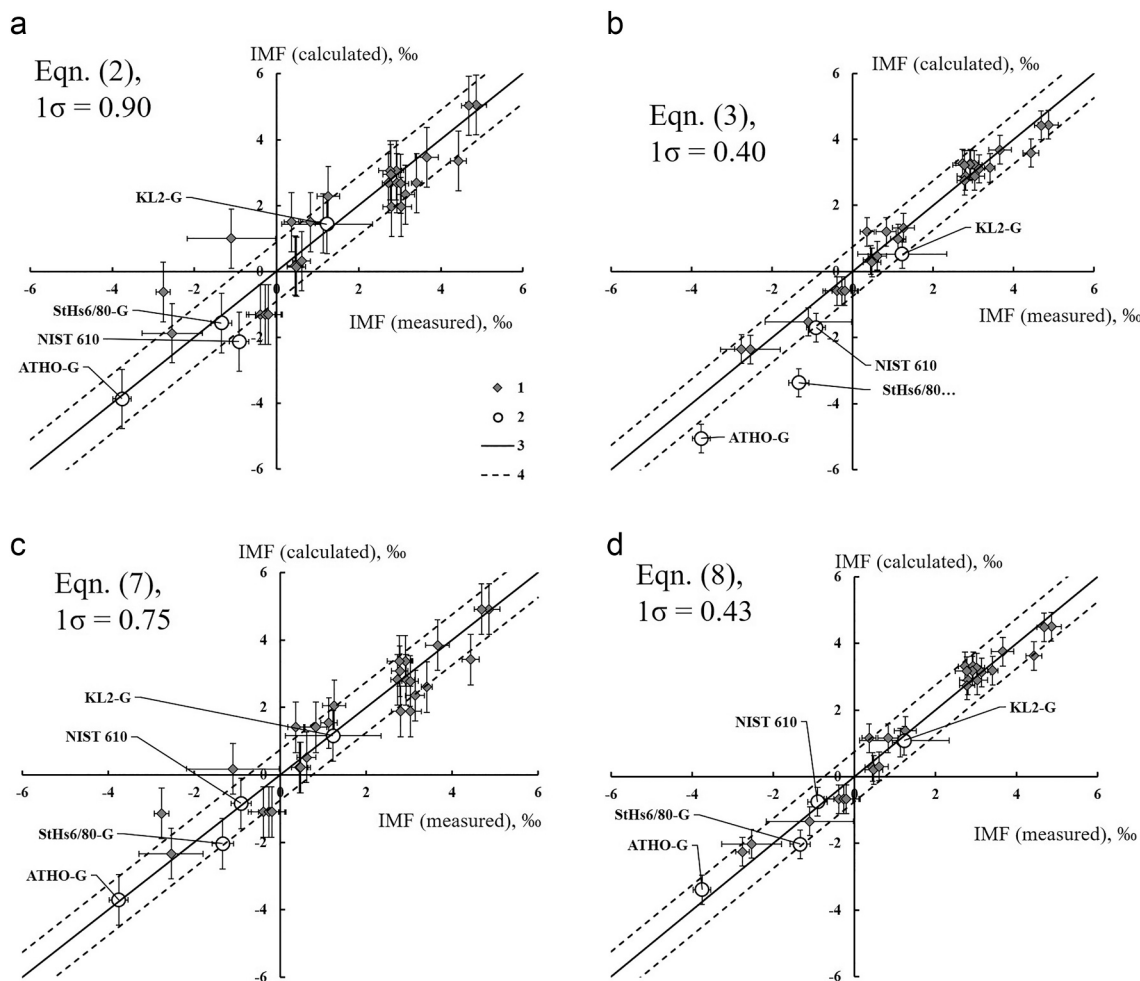
Fig. 6. Predicted IMF values in SAFCMT and standard glasses vs. true IMF values obtained by SIMS and laser fluorination GS IRMS analyses. Predictions were made using the Eqs. (2), (3), (7), and (8) (figures a, b, c, and d respectively). Uncertainty estimates correspond to 1σ from the Table 4 for IMF calculated and combined error of SIMS and laser fluorination analyses for IMF measured. Notations: 1 – SAFCMT glasses, 2 – standard and natural glasses (MPI-DING and NIST 610), 3 – 1:1 line, 4 – the 1σ interval around the 1:1 line.
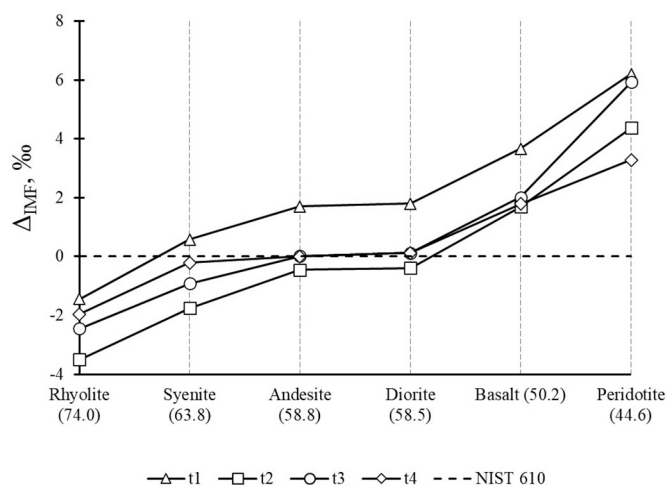

Fig. 7. Predicted Δ_{IMF} values (difference in IMF calculated for glass matrixes with the hypothetical natural rock compositions and reference material NIST 610). Major elements compositions for numerous rock types were taken from Zhao and Zheng (2003) after Le Maitre (1976).

reference material (i.e., Δ_{IMF}) where

$$\Delta_{IMF} = (IMF_{Rock} - IMF_{NIST\ 610}) \tag{9}$$

In Fig. 7 the Δ_{IMF} values calculated using the models based on Eqs. (2), (3), (7), and (8) are compared. The Δ_{IMF} values can vary up to 7 or 8‰ when glass composition span the range from rhyolite to peridotite. The model based solely on SiO_2 contents (Eq. (2)) yields Δ_{IMF} values which are systematically higher than ones obtained using models based on the Eqs. (3), (7), and (8). All models predict that basic and ultra-basic glasses should yield large positive bias relative to NIST 610. Comparing the SiO_2 single oxide model with three other models suggests that consideration of the contributions of all major element oxides, especially with particularly large or particularly small cation radii, is necessary in order to predict an accurate IMF correction.

5. Conclusions

SIMS measurements of 27 experimental glasses with differing contents of six major oxides, run during a single continuous SIMS session, allow us to confirm that SIMS oxygen isotope matrix effects in silicate glasses are strongly depend on a given material's chemical composition. The prediction of IMF based on the chemical-depend isotope I-^{18}O index shows that cation-oxygen bond strength influences the IMF in silicate glasses.

A subsequent analytical test assessed the reliability of our four

models; each of which showed advantages and disadvantages. We have confirmed that SiO_2 concentrations can be used to predict IMF values, as has been proposed in earlier studies (Hartley et al., 2012; Gurenko et al., 2001; Gurenko and Chaussidon, 2002), but also that this model is not suitable for glasses rich in large-cation and alkaline elements, including NIST 610. Furthermore, the SiO_2-correction Eq. (2) has a large standard error of nearly ±0.9‰, though it does correctly predict the oxygen isotope values of the three natural MPI-DING glasses at better than the ±0.3‰ level.

Eq. (3) predicts IMF at near ±0.4‰ and we have shown that it can be applied to alkaline-poor and even alkaline-free glasses. This equation poorly predicts the $\delta^{18}O$ values of natural glasses (offset from GS-MS results from 0.7 to 2‰) that contain oxides such as Na_2O and K_2O that are not considered by this equation. We conclude that empirical-based IMF models will be more successful if they include the alkali-oxides as shown by our modified model Eq. (8). Eq. (8) predicts the IMF values of all glasses reasonably well and has the standard error (±0.43‰), but empirical coefficients d_i at X_{Na2O} and X_{K2O} are poorly defined, signaling a need for additional reference materials containing these two elements. An additional study of alkali-rich glasses is highly desirable.

We found a strong correlation ($R^2 = 0.87$) between IMF values and the I-^{18}O index. Our Eq. (7) works well for all standard glasses, including the Na-rich material NIST 610. This equation has a lower standard error (±0.75‰) than SiO_2-correction Eq. (2) and predicts IMF in three of five alkali-bearing glasses to within 0.06–0.12‰, thus achieving the data quality of the GS-MS laser fluorination technique. In the absence of experimental IMF calibrations for glasses containing alkaline and large-ion elements, the I-^{18}O index can be recommended to correct the SIMS data for natural and artificial glasses with complex compositions.

Declaration of Competing Interest

The authors declare that they have no known competing financial interests or personal relationships that could have appeared to influence the work reported in this paper.

Acknowledgements

Appendix A. Supplementary data

Supplementary data to this article can be found online at https://doi.org/10.1016/j.chemgeo.2021.120322.

References

Baertschi, P., 1976. Absolute ^{18}O content of standard mean ocean water. Earth and Planetary Science Letters 31 (3), 341–344.

Balestra, B., Orland, I.J., Fessenden-Rahn, J., Gorski, G., Franks, R., Rahn, T., Paytan, A., 2020. Paired analyses of oxygen isotope and elemental ratios within individual shells of benthic foraminifera genus Uvigerina. Chem. Geol. 533, 119377.

Bindeman, I., 2008. Oxygen isotopes in mantle and crustal magmas as revealed by single crystal analysis. Rev. Mineral. Geochem. 69, 445–478.

Borisov, A.A., Dubinina, E.O., 2014. Effect of network-forming cations on the oxygen isotope fractionation between silicate melts: Experimental study at 1400–1570 °C. Petrology 22, 359–380.

Borisov, A., Behrens, H., Holtz, F., 2013. The effect of titanium and phosphorus on ferric/ferrous ratio in silicate melts: an experimental study. Contrib. Mineral. Petrol. 166, 1577–1591.

Borisov, A., Behrens, H., Holtz, F., 2015. Effects of melt composition on Fe^{3+}/Fe^{2+} in silicate melts: a step to model ferric/ferrous ratio in multicomponent systems. Contrib. Mineral. Petrol. 169, 24.

Borisov, A., Behrens, H., Holtz, F., 2017. Effects of strong network modifiers on Fe^{3+}/Fe^{2+} in silicate melts: an experimental study. Contrib. Mineral. Petrol. 172, 34.

Borisov, A., Behrens, H., Holtz, F., 2018. Ferric/ferrous ratio in silicate melts, a new model for 1 atm data with special emphasis on the effects of melt composition. Contrib. Mineral. Petrol. 173, 98.

Busch, K.L., Hsu, B.H., Xie, Y.-X., Cooks, R.G., 1983. Matrix effects in secondary ion mass spectrometry. Anal. Chem. 55, 1157–1160.

Chakraborty, P., 1998. Secondary ion mass spectrometry for quantitative surface and in-depth analysis of materials. Pramana J. Phys. 50, 617–640.

Dargie, M., Winckler, G., Gröning, M., 2007. In: Coplen, T.B., Vocke, R.D. (Eds.), NBS 28 & NBS 30 Updated Reference Sheet on an Earlier NIST Report of Investigation. IAEA issued: 11 April 2007.

Davies, J.H.F.L., Stern, R.A., Heaman, L.M., Moser, D.E., Walton, E.L., Vennemann, T., 2018. Evaluating baddeleyite oxygen isotope analysis by secondary ion mass-spectrometry (SIMS). Chem. Geol. 479, 113–122.

Deegan, F.M., Whitehouse, M.J., Troll, V.R., Budd, D.A., Harris, C.G., Harri, H.U., 2016. Pyroxene standards for SIMS oxygen isotope analysis and their application to Merapi volcano, Sunda arc, Indonesia. Chem. Geol. 447, 1–10.

Deline, V.R., Katz, W., Evans, C.A., Williams, P., 1978. Mechanism of the SIMS matrix effect. Appl. Phys. Lett. 33, 832–835.

Dubinina, E.O., Borisov, A.A., 2018. Structure and composition effects on the oxygen isotope fractionation in silicate melts. Petrology 26, 414–427.

Eiler, J.M., 2001. Oxygen isotope variations of basaltic lavas and upper mantle rocks. In: Valley, J.W., Cole, D.R. (Eds.), Stable Isotope Geochemistry, Rev. Mineral, 43, pp. 319–364.

Eiler, J.M., Graham, C., Valley, J.W., 1997. SIMS analysis of oxygen isotopes: matrix effects in complex minerals and glasses. Chem. Geol. 138, 221–244.

Fàbrega, C., Parcerisa, D., Rossell, J.M., Gurenko, A., Franke, C., 2017. Predicting instrumental mass fractionation (IMF) of stable isotope SIMS analyses by response surface methodology (RSM). J. Anal. At. Spectrom. 32, 695–860.

Franchi, I.A., Wright, I.P., Sexton, A.S., Pillinger, C.T., 1999. The oxygen-isotopic composition of Earth and Mars. Meteorit. Planet. Sci. 34, 657–661.

Fukuda, K., Beard, B.L., Dunlap, D.R., Spicuzza, M.J., Fournelle, J.H., Wadhwa, M., Kita, N., 2020. Magnesium isotope analysis of olivine and pyroxene by SIMS: Evaluation of matrix effect. Chem. Geol. 540, 119482.

Gurenko, A., Chaussidon, M., 2002. Oxygen isotope variations in primitive tholeiites of Iceland: evidence from a SIMS study of glass inclusions, olivine phenocrysts and pillow rim glasses. Earth Planet. Sci. Lett. 205, 63–79.

Gurenko, A., Chaussidon, M., Schmincke, H.-U., 2001. Magma ascent and contamination beneath one intraplate volcano: evidence from S and O isotopes in glass inclusions and their host clinopyroxenes from Miocene basaltic hyaloclastites southwest of Gran Canaria (Canary Islands). Geochim. Cosmochim. Acta 65, 4359–4374.

Hartley, M.E., Thordarson, T., Taylor, C., Fitton, J.G., EIMF, 2012. Evaluation of the effects of composition on instrumental mass fractionation during SIMS oxygen isotope analyses of glasses. Chem. Geol. 334, 312–323.

Hauri, E., Wang, J., Dixon, J.E., King, P.L., Mandeville, C., Newman, S., 2002. SIMS analysis of volatiles in silicate glasses 1. Calibration, matrix effects and comparisons with FTIR. Geology 183, 99–114.

Hauri, E.H., Shaw, A.M., Wang, J., Dixon, J.E., King, P.L., Mandeville, C., 2006. Matrix effects in hydrogen isotope analysis of silicate glasses by SIMS. Chem. Geol. 235, 352–365.

Hinton, R.W., 1995. Ion microprobe analysis in geology. In: Potts, P.J., Bowles, J.W.F., Reed, S.J.B., Cave, M.R. (Eds.), Microprobe Techniques in the Earth Sciences, pp. 235–289. London.

Hinton, R.W., 1999. NIST SRM 610, 611 and SRM 612, 613 multi-element glasses: constraints from element abundance ratios measured by microprobe techniques. Geostand. Newslett. 23 (2), 197–207.

Hoffbauer, R., Hoernes, S., Fiorentini, E., 1994. Oxygen isotope thermometry based on a refined increment method and its application to granulite-grade rocks from Sri Lanka. Precambrian Res. 66, 199–220.

Huberty, J.M., Kita, N.T., Kozdon, R., Heck, P.R., Fournelle, J.H., Spicuzza, M.J., Xu, H., Valley, J.W., 2010. Crystal orientation effects in $\delta^{18}O$ for magnetite and hematite by SIMS. Chem. Geol. 276, 269–283.

Ickert, R.B., Stern, R.A., 2013. Matrix Corrections and Error Analysis in High-Precision SIMS$^{18}O/^{16}O$ Measurements of Ca–Mg–Fe Garnet. Geostand. Geoanaly. Res. 37 (4), 429–448.

Ickert, R.B., Hiess, J., Williams, I.S., Holden, P., Ireland, T.R., Lanc, P., Schram, N., Foster, J.J., Clement, S.W., 2008. Determining high precision, in situ, oxygen isotope ratios with a SHRIMP II: analyses of MPI-DING silicate-glass reference materials and zircon from contrasting granites. Chem. Geol. 257, 114–128.

Isa, J., Kohl, I.E., Liu, M.-C., Wasson, J.T., Young, E.D., McKeegan, K.D., 2017. Quantification of oxygen isotope SIMS matrix effects in olivine samples: Correlation with sputter rate. Chem. Geol. 458, 14–21.

Jochum, K.P., et al., 2006. MPI-DING reference glasses for in situ microanalysis: New reference values for element concentrations and isotope ratios. Geochem. Geophys. Geosyst. 7, Q02008 https://doi.org/10.1029/2005GC00106.

Kasemann, S., Meixner, A., Rocholl, A., Vennemann, T., Rosner, M., Schmitt, A.K., Wiedenbeck, M., 2001. Boron and oxygen isotope composition of certified reference materials NIST SRM 610/612 and reference materials JB-2 and JR-2. Geostand. Newslett. 25, 405–416.

Kita, N.T., Ushikubo, T., Fu, B., Valley, J.W., 2009. High precision SIMS oxygen isotope analysis and the effect of sample topography. Chem. Geol. 264, 43–57.

Kusakabe, M., Maruyama, S., Nakamura, T., Yada, T., 2004. CO_2 laser-BrF_5 fluorination technique for analysis of oxygen three isotopes of rocks and minerals. J. Mass Spectrom. Soc. Jpn 52, 205–212.

Le Maitre, R.W., 1976. The chemical variability of some common magmatic rocks. J. Petrol. 17, 589–637.

Mysen, B.O., Richet, P., 2005. Silicate Glasses and Melts: Properties and Structure. Elsevier, Amsterdam, 548 pp.

Ottolini, L., Cámara, F., Hawthorne, F.C., Stirling, J., 2002. SIMS matrix effects in the analysis of light elements in silicate minerals: comparison with SREF and EMPA data. Am. Mineral. 87, 1477–1485.

Page, F.Z., Kita, N.T., Valley, J.W., 2010. Ion microprobe analysis of oxygen isotopes in garnets of complex chemistry. Chem. Geol. 270, 9–19.

Pearce, N.J.G., Perkins, W.T., Westgate, J.A., Gorton, M.P., Jackson, S.E., Neal, C.R., Chenery, S.P., 1997. A compilation of new and published major and trace element data for NIST SRM 610 and NIST SRM 612 Glass reference materials. Geosand. Newslett. 21, 115–144.

Riciputi, L.R., Paterson, B.A., Ripperdan, R.L., 1998. Measurement of light stable isotope ratios by SIMS: matrix effects for oxygen, carbon, and sulfur isotopes in minerals. Int. J. Mass Spectrom. 178, 81–112.

Rollion-Bard, C., Marin-Carbonne, J., 2011. Determination of SIMS matrix effects on oxygen isotopic compositions in carbonates. J. Anal. At. Spectrom. 26, 1285–1289.

Rosner, M., Wiedenbeck, M., Ludwig, T., 2008. Composition-induced variations in SIMS instrumental mass fractionation during boron isotope ratio measurements of silicate glasses. Geostand. Geoanal. Res. 32 (1), 27–38.

Schütze, H., 1980. Der Isotopenindex - eine Inkrementenmethode zur näherungsweisen Berechnung von Isotopenaustauschgleichgewichten zwischen kristallinen Substanzen. Chem. Erde 39, 321–334.

Scicchitano, M.-R., Rubatto, D., Hermann, J., Majumdar, A.S., Putnis, A., 2018. Oxygen isotope analysis of olivine by ion microprobe: matrix effects and applications to a serpentinised dunite. Chem. Geol. 499, 126–137.

Shannon, R.D., 1976. Revised effective ionic radii and systematic studies of interatomic distances in halides and chalcogenides. Acta Crystallogr. A32, 751–767.

Sharp, Z.D., 1990. A laser-based microanalytical method for the in-situ determination of oxygen isotope ratios in silicates and oxides. Geochim. Cosmochim. Acta 54, 1353–1357.

Shimizu, N., 1986. Silicon-induced enhancement in secondary ion emission from silicates. Int. J. Mass Spectrom. Ion Process. 69, 325–338.

Šliwiñski, M.G., Kitajima, K., Spicuzza, M.J., Orland, I.J., Ishida, A., Fournelle, J.H., Valley, J.W., 2018. SIMS bias on isotope ratios in Ca-Mg-Fe carbonates (Part III): $\delta^{18}O$ and $\delta^{13}C$ matrix effects along the magnesite–siderite solid-solution series. Geostand. Geoanal. Res. 42 (1), 49–76.

Sun, Yadong, Wiedenbeck, Michael, Joachimski, Michael, Beier, Christoph, Kemner, Fabian, Weinzierl, Christoph, et al., 2016. Chemical and oxygen isotope composition of gem-quality apatites: Implications for oxygen isotope reference materials for secondary ion mass spectrometry (SIMS). Chemical Geology 440, 164–178. https://doi.org/10.1016/j.chemgeo.2016.07.013.

Valley, J.W., 2001. Stable isotope thermometry at high temperatures. Rev. Mineral. Geochem. 43, 365–414.

Valley, J.W., Kitchen, N., Kohn, M.J., Niendorf, C.R., Spicuzza, M.J., 1995. UWG-2, a garnet standard for oxygen isotope ratios: strategies for high precision and accuracy with laser heating. Geochim. Cosmochim. Acta 59, 5223–5231.

Vielzeuf, D., Champenois, M., Valley, J.W., Brunet, F., Devidal, J.L., 2005. SIMS analyses of oxygen isotopes: matrix effects in Fe–Mg–Ca garnets. Chem. Geol. 223, 208–226.

Zhao, Z.F., Zheng, Y.F., 2003. Calculation of oxygen isotope fractionation in magmatic rocks. Chem. Geol. 193, 59–80.

Zheng, Y.-F., 1991. Calculation of oxygen isotope fractionation in metal oxides. Geochim. Cosmochim. Acta 55, 2299–2307.

Zheng, Y.F., 1993. Calculation of oxygen isotope fractionation in anhydrous silicate minerals. Geochim. Cosmochim. Acta 57, 1079–1091.

Zheng, Y.-F., 1999. Calculation of oxygen isotope fractionation in minerals. Episodes 22, 99–106.